Pergamon

Int. J. Heat Mass Transfer. Vol. 38, No. 4, pp. 691–700, 1995

0017-9310/95 $9.50+0.00

0017-9310(94)00191-X

Mass transfer from a sublimating naphthalene flat plate to a parallel flow of air

NAJI J. NASSIF
Gnesys, Inc., Southaven, MS 38671, U.S.A.

WILLIAM S. JANNA†
Department of Mechanical Engineering, Memphis State University, Memphis, TN 38152, U.S.A.

and

GERALD S. JAKUBOWSKI
College of Engineering and Science, Loyola Marymount University, Los Angeles, CA 90045, U.S.A.

(*Received* 4 *January* 1994 *and in final form* 10 *June* 1994)

Abstract—Naphthalene sublimation was used to experimentally determine the average mass transfer coefficient in parallel, turbulent flow of air over a flat plate having a step discontinuity. Transfer coefficients were collected for Reynolds numbers ranging from approximately 40 000 to 2 000 000. Data were compared to a semi-empirical relationship based on the $1/n$ power law. A formulation was devised involving the Schmidt number as an integral part of the solution, thus avoiding Reynolds' analogy. The Schmidt number exponent and the power profile coefficient were expressed in terms of n, which makes the mass transfer coefficient directly obtainable from the Reynolds number.

INTRODUCTION

The topic of this paper is flow over a flat plate, a portion of which sublimates. The sublimating substance is naphthalene. The objective of the work is to obtain data on average mass transfer coefficients and to formulate a new method of correlating the results.

Local mass transfer coefficients from a flat plate have been extensively investigated. However, little attention has been given to correlating the proposed average mass transfer coefficient solutions to collected data.

Maisel and Sherwood [1] collected mass transfer data from a porous flat plate using water. The Reynolds number ranged from 65 000 to 674 000 and the data were correlated to friction coefficient equations according to the Chilton–Colburn analogy.

Scesa and Sauer [2] ran tests of heat transfer in turbulent flow over a flat plate with a stepwise discontinuous surface temperature using heated strips. They applied the Rubesin starting length correction to correlate their data with the Colburn analogy. Their results showed good correlation with Rubesin's starting length correction for Reynolds numbers between 60 000 and 800 000.

Sherwood and Bryant [3] used naphthalene to determine sublimation mass transfer from flat plates in compressible boundary layers with a reported Mach number of 0.43 for the incompressible case. Incompressible flow theory has been found to generate an error of approximately 10% in the density prediction at such a Mach number [4].

Sogin [5] used naphthalene cast in trays to simulate isothermal strips on a 0.38 m (15″) flat plate. The tests were run under laminar flow conditions. The majority of the data were collected at a Reynolds number of 250 000. Sogin reported good agreement with laminar flow theory. In a follow-up publication, Sogin and Goldstein [6] used the same set-up in turbulent flow. A thin wire was used to trip the boundary layer. The tests were performed at two free stream velocities: 22.6 and 34.1 m s^{-1} (74 and 112 ft s^{-1}). The range of the Reynolds number extended from 150 000 to 500 000. Due to the existence of the trip wire, the origin of the boundary layer was estimated to be 0.05 m (2″) upstream of the leading edge. This apparent location was then used as the origin for all measurements along the plate.

Reynolds [7] proposed a solution for the heat transfer from a flat plate in turbulent flow with a step change in temperature. While his was not the first, it provided better correlation than previous methods. Reynolds reported that while his own data behaved similarly to Scesa and Sauer's for the same range of

† Author to whom correspondence should be addressed.

NOMENCLATURE

C_A	local naphthalene concentration [mol m^{-3}]
C_{A0}	naphthalene concentration at soluble surface [mol m^{-3}]
$C_{A\infty}$	free stream naphthalene concentration [mol m^{-3}]
$c_f/2$	local skin friction coefficient, $\tau_0/\rho v_\infty^2$
$\mathscr{D}_{AB}$	binary diffusivity of naphthalene into air [m^2 s^{-1}]
H	height of laboratory [m]
$\bar{h}_{mL}$	average mass transfer coefficient [m s^{-1}]
$\bar{h}_{mx}$	local mass transfer coefficient [m s^{-1}]
L	length of flat plate [m]
$\mathscr{L}$	length of naphthalene cast [m]
l	length of laboratory [m]
m_f	final mass of plate for the actual test [kg]
m_{ft}	final mass of plate for the transient losses test [kg]
m_{in}	initial mass of plate for the actual test [kg]
m_{int}	initial mass of plate for the transient losses test [kg]
n	denominator of power in power profile
N_A	molar flux [mol m^{-2} s^{-1}]
Re_L	overall Reynolds number, $v_\infty L/\nu$
Re_x	local Reynolds number, $v_\infty x/\nu$
Sc	Schmidt number, $\nu/\mathscr{D}_{AB}$
Sh	Sherwood number, $Sc\,\bar{h}_{mL}L/\nu$
St_{AB_L}	average Stanton number, $\bar{h}_{mL}/v_\infty$
St_{AB_x}	local binary Stanton number, $\bar{h}_{mx}/v_\infty$ or $d\delta_4/dx$
St	local Stanton number for heat transfer, $\bar{h}_x/v_\infty$
t	duration of a single actual test run [s]
T_{av}	average absolute temperature during a test run [K]
v_∞	free stream velocity [m s^{-1}]
v_x	x-component of velocity [m s^{-1}]
v_x^+	x-component of universal velocity, $v_x/(\tau_0/\rho)^{1/2}$
W	width of naphthalene cast [m]
w	width of laboratory [m]
x	distance along the plate from the leading edge [m]
x_0	location of the concentration step change [m]
y	distance away from the plate [m]
y^+	universal distance away from the plate, $y(\tau_0/\rho)^{1/2}/\nu$.

Greek symbols

Δ	ratio of concentration boundary layer thickness to momentum boundary layer thickness
δ	momentum boundary layer thickness [m]
δ_2	momentum thickness [m]
δ_4	diffusion thickness [m]
δ_c	diffusion (or concentration) boundary layer thickness [m]
ε_c	eddy concentration diffusivity [m^2 s^{-1}]
ε_m	eddy momentum diffusivity [m^2 s^{-1}]
λ	coefficient of $1/n$ velocity power profile
ν	kinematic viscosity, i.e. momentum diffusivity of free stream fluid [m^2 s^{-1}]
ρ	density of free stream fluid [kg m^{-3}]
ρ_{v_s}	free stream vapor density of sublimating substance [kg m^{-3}]
ρ_{v_∞}	surface vapor density of sublimating substance [kg m^{-3}]
τ_0	shear stress at the wall, $-\mu(\partial v_x/\partial y)\vert_0$ [N m^{-2}]
τ_y	shear stress at a distance y inside the boundary layer [N m^{-2}].

Reynolds numbers, the Rubesin starting length correction became inadequate at higher Reynolds numbers, especially near the temperature discontinuity. He based his velocity and temperature profiles on the $1/n$ power law and used the Reynolds analogy to relate heat diffusivity to momentum diffusivity, hence limiting his solution to Prandtl numbers of 1. Despite the fact that his velocity and temperature profiles over his flat plate coincide with $n = 5.6$, he used a value of $n = 7$ because it correlated much better with his heat transfer data. He had experimental agreement with his solution up to a Reynolds number of 3 500 000.

Recently, there has been a renewed interest in 1/7 power law for predicting heat transfer from flat plates. Love *et al.* [8, 9] and Taylor *et al.* [10] repeated Reynolds' experiment. However, they used the bottom wall of the test section as their heated plate. A thin wire was used to trip the boundary layer. They were able to duplicate Reynolds' results and extend the validity of the 1/7 power law to a Reynolds number of 10 000 000.

Chyou [11] used the 1/7 power law based on Reynolds' work to obtain an analytical solution for the special case of a constant heat flux plate with a short unheated insert containing a concentrated heat source. He compared his solution to data and to a numerical model. He concluded that the analytical method provides a simple, technically useful tool for predicting heat transfer from flat plates in turbulent flows.

Huang *et al.* [12] constructed mean velocity profiles

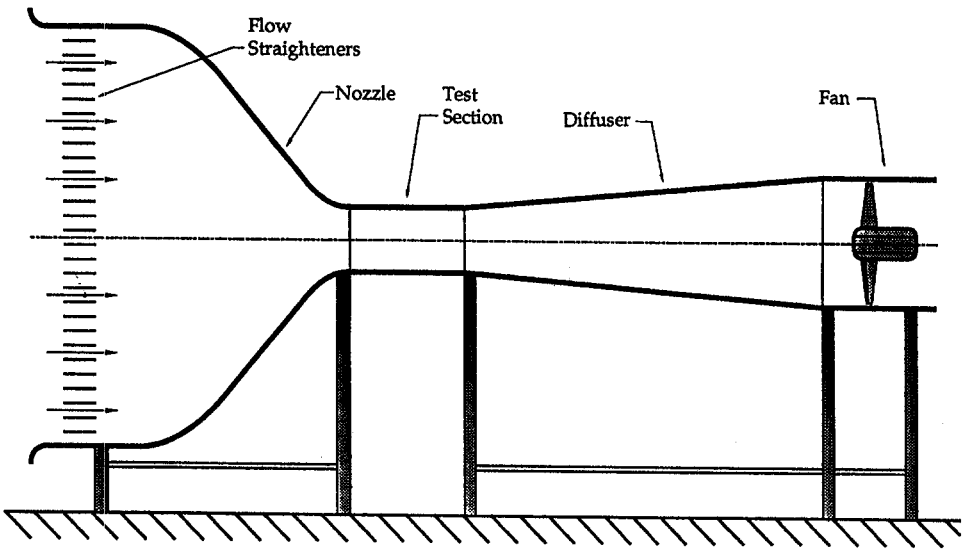

Fig. 1. Section view of open loop wind tunnel.

for turbulent boundary layers with isothermal or adiabatic walls. The Prandtl number was assumed to be 0.9 throughout the study. A good agreement with data is obtained for Mach numbers as high as 11. This paper proposes an iterative technique for determining the skin friction and, while it studies the effects of a temperature difference between the surface of the plate and the free stream on the shape factor, it does not discuss heat transfer coefficients.

So [13] studied the effects of the pressure gradient on turbulent heat transfer to or from planar surfaces under incompressible, equilibrium thermal boundary layers. At incipient separation, a modified Reynolds analogy that accounts for the turbulent Prandtl number and the equilibrium condition is deduced and finite limitations on the validity of the classical Reynolds analogy are placed, i.e. the turbulent Prandtl number must be between 0.7 and 2. His solution is based on the logarithmic law of the wall and the defect law of the outer region, and is obtained through a numerical fourth-order Runge–Kutta technique followed by a predictor corrector method.

In this study, mass transfer data are collected to investigate the average mass transfer coefficient as opposed to the more extensively investigated local mass transfer coefficient. Moreover, a semi-empirical solution method based on the $1/n$ power profile is suggested, in which the Reynolds analogy is circumvented and the Schmidt number, the power n, and the universal velocity coefficient λ are related to the Reynolds number.

APPARATUS AND PROCEDURE

A subsonic low-speed open-loop wind tunnel having a cross-section of 0.61×0.61 m (2×2 ft) and 0.91 m (3 ft) long was used in this study (Fig. 1.) The wind tunnel was equipped with a 40 hp variable pitch fan providing a maximum speed of approximately 46 m s^{-1} (150 ft s^{-1}). The wind tunnel comes equipped with a Pitot probe rack having axial and vertical degrees of freedom. The Pitot probe was connected to an inclined manometer.

Temperature was recorded via two unshielded type-K chromel–alumel thermocouples. The scale used for weighing the flat plate was a Mettler PM6100. It has a range of 6.1 kg (13.3 lbm) and increments of 0.000 1 kg (0.0001 lbm) (see Fig. 2 for more detail about experimental set-up). While Figs. 1 and 2 show the leading edge of the plate to be right past the nozzle contraction, in actuality this contraction is much less abrupt, such that the leading edge is approximately 66 cm (2 ft) from any noticeable change in slope of the nozzle.

The naphthalene surface was cast in a recessed aluminum plate 64 cm (26″) long, 34.29 cm (13.5″) wide and 1.27 cm (0.5″) thick. The recess was 0.64 cm (0.25″) deep and 5.1 cm (2″) from the leading edge (see Fig. 3). Four different naphthalene plate lengths were cast and tested at different velocities to increase the range of the Reynolds number. The average mass transfer coefficients were estimated by determining the change in mass of the naphthalene plate over a measured time period for a given speed. Transient mass losses were experimentally determined prior to each run. The naphthalene used in the different casts was Scintillation Grade +99% pure. It has a melting point of approximately 80.5°C (176.9°F). The casting method used gave a smooth glass-like naphthalene surface.

Due to the start-up time required for the fan to reach steady state and the time required for the manometer to stabilize, the naphthalene transient mass losses needed to be accounted for and subtracted from the steady-state results of the test. Prior to each run,

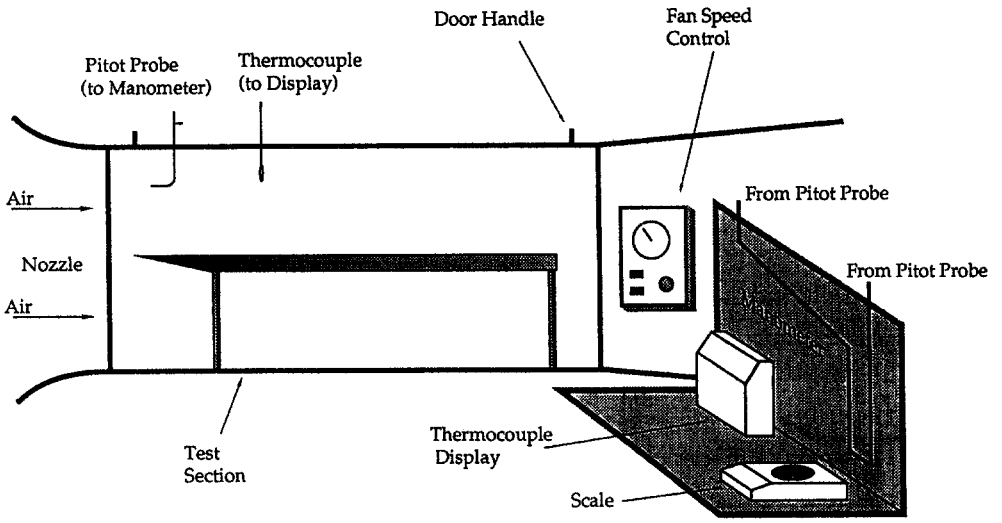

Fig. 2. Schematic of test set-up.

the plate was weighed and placed in the wind tunnel. The wind tunnel fan was then started, the manometer was allowed to stabilize at the pre-established setting and then the fan was immediately shut-off. The plate was re-weighed. The change in weight was recorded. The plate was re-installed in the wind tunnel at which time the procedure was repeated for a desired period at the end of which the plate was re-weighed. Temperature readings were taken at the beginning and completion of each test.

THEORY

Consider flow over a sublimating flat plate as shown in Fig. 4. The flow is steady and the plate is parallel to the flow. The Von Karman–Pohlhausen boundary layer solution for steady, incompressible, isothermal, parallel flow over a sublimating flat plate with no chemical reactions is:

$$v_\infty^2 \frac{\partial \delta_2}{\partial x} = \nu \left.\frac{\partial v_x}{\partial y}\right|_0$$

where

$$\delta_2 = \int_0^\infty \left[\frac{v_x}{v_\infty}\left(1 - \frac{v_x}{v_\infty}\right)\right] \mathrm{d}y \tag{1}$$

with

$$N_A|_{y=0} = \frac{\mathrm{d}}{\mathrm{d}x}[v_\infty (C_{A_0} - C_{A_\infty})\delta_4] \tag{2}$$

where

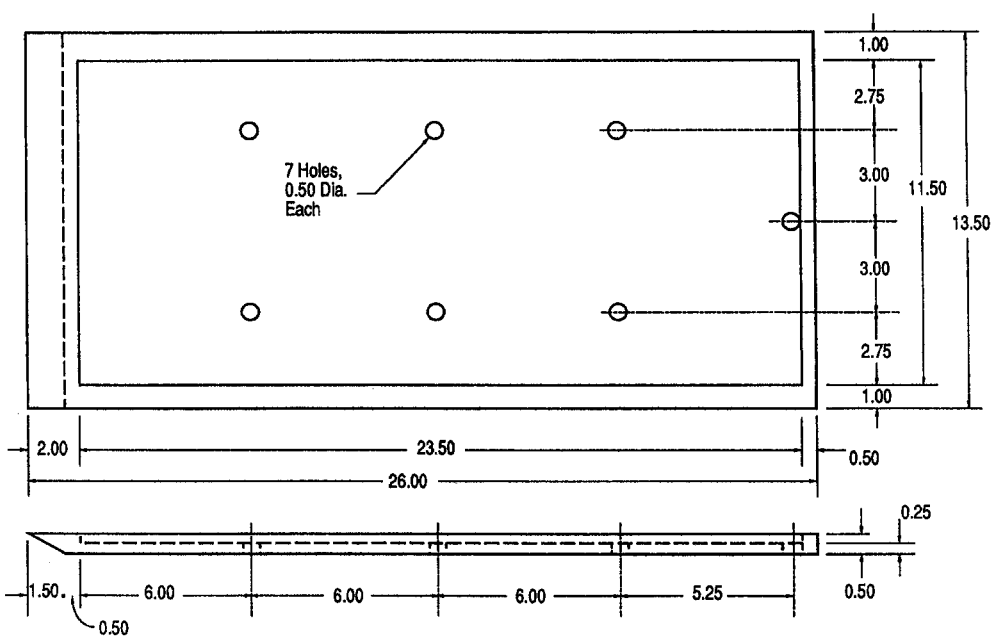

Fig. 3. Schematic of flat plate (not to scale). All dimensions in inches.

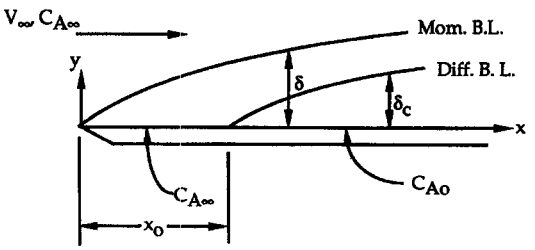

Fig. 4. Schematic of the boundary layer problem.

$$N_A|_{y=0} = -\mathscr{D}_{AB}\frac{\partial C_A}{\partial y}\bigg|_0$$

and

$$\delta_4 = \int_0^\infty \frac{v_x}{v_\infty}\left[1-\frac{C_{A_0}-C_A}{C_{A_0}-C_{A_\infty}}\right]dy.$$

The modified boundary conditions are:

BC1: $v_x = 0$ at $y = 0$

BC2: $v_x = v_\infty$ at $y = \delta$

BC3: $v_x = v_\infty$ at $x = 0$

BC4: $\dfrac{\partial v_x}{\partial y} = 0$ at $y = \delta$

BC5: $C_A = C_{A_0}$ at $y = 0$ $x \geqslant x_0$

BC6: $C_A = C_{A_0}$ at $x = x_0$ $y = 0$

BC7: $C_A = C_{A_\infty}$ at $y = \delta$

BC8: $\dfrac{\partial C_A}{\partial y} = 0$ at $y = \delta$.

For turbulent flow, a $1/n$ power profile will be assumed for both the velocity and the concentration inside their respective boundary layers. Hence, the universal velocity profile can be written as a function of the universal distance from the flat plate as:

$$v_x^+ = \lambda(y^+)^{1/n} \tag{3}$$

where λ is a positive real number. Replacing v_x^+ and y^+ by their definitions, applying BC2 and obtaining the ratio between the general equation and its value at the boundary condition, yields:

$$\frac{v_x}{v_\infty} = \left(\frac{y}{\delta}\right)^{1/n}. \tag{4}$$

Substituting the definition of the shear stress at the wall into equation (1) and rearranging, after some mathematical manipulations, yields:

$$\frac{c_f}{2} = \left[\lambda^n\frac{(n+2)(n+3)}{n}Re_x\right]^{-2/(n+3)}. \tag{5}$$

Applying BC2 to equation (3), solving for τ_0 and replacing in the definition of the friction coefficient, yields:

$$\frac{c_f}{2} = \frac{\tau_0}{\rho v_\infty^2} = \left[\lambda^n\frac{v_\infty\delta}{\nu}\right]^{-2/(n+1)}. \tag{6}$$

Because the flow is turbulent, the shear stress must be defined so as to account for the turbulent contributions [14]. Hence,

$$\frac{\tau_y}{\rho} = (\nu+\varepsilon_m)\frac{\partial v_x}{\partial y}. \tag{7}$$

After some mathematical manipulations, the total turbulent viscosity becomes

$$(\nu+\varepsilon_m) = n\nu\frac{c_f}{2}\frac{\delta}{x}Re_x\left[1-\left(\frac{y}{\delta}\right)^{(n+2)/n}\right]\left(\frac{y}{\delta}\right)^{(n-1)/n}. \tag{8}$$

For a trace concentration, the molar flux can be defined as [15]:

$$N_A = -(\mathscr{D}_{AB}+\varepsilon_c)\frac{\partial C_A}{\partial y}. \tag{9}$$

Again, using a $1/n$ relationship, the concentration profile is:

$$\frac{C_{A_0}-C_A}{C_{A_0}-C_{A_\infty}} = \left(\frac{y}{\delta_c}\right)^{1/n}. \tag{10}$$

Replacing equation (9) into equation (8) yields:

$$N_A = (\mathscr{D}_{AB}+\varepsilon_c)(C_{A_0}-C_{A_\infty})\frac{1}{n\delta_c^{1/n}}y^{(1-n)/n}. \tag{11}$$

At this stage, a relationship between the total mass and momentum diffusivities is required. Reynolds *et al.* [16], in the solution to the heat transfer counterpart to this problem, proposed that the Reynolds analogy be used. The Reynolds analogy states that both the molecular and turbulent Prandtl numbers are equal to unity, thus yielding a total Prandtl number equal to unity. This is a shortcoming of the solution since it omits the Prandtl number effects and renders it invalid for fluids having a Prandtl number other than 1. For heat transfer in air, this may not be a problem since the molecular and turbulent Prandtl numbers for air are approximately 0.7 and 0.9, respectively. It is necessary, however, to modify this approach to make it appropriate for the more general case.

Applying the Reynolds analogy to the mass transfer solution yields:

$$Sc = 1.$$

However, the Schmidt number for naphthalene is 2.5 [5]. It is suggested in this study that the molecular Schmidt number raised to a power α be set equal to the ratio of the total momentum and binary diffusivities, such that:

$$Sc^\alpha = \frac{\nu+\varepsilon_m}{\mathscr{D}_{AB}+\varepsilon_c} \tag{12}$$

where α will be determined empirically. The nature of α, i.e. a real constant or a variable, will be established later in this paper.

Combining equations (7) and (9)–(11) yields:

$$St_{AB_x} = \frac{1}{Sc^{\alpha}} \frac{c_f}{2} \left(\frac{\delta}{\delta_c}\right)^{1/n}. \quad (13)$$

The use of α gives the binary Stanton number as a function of the Schmidt number. The Stanton number is defined as the gradient of the diffusion thickness in the streamwise direction [14], such that:

$$St_{AB_x} = \frac{d\delta_4}{dx}. \quad (14)$$

Applying the above definition for the Stanton number, and making the necessary substitutions into equation (12), yields:

$$\frac{c_f}{2} = \frac{n\,Sc^{\alpha}}{(n+1)(n+2)} \left(\frac{\delta_c}{\delta}\right)^{1/n} \frac{d}{dx}\left[\delta_c \left(\frac{\delta_c}{\delta}\right)^{1/n}\right] \quad (15)$$

where the newly proposed Sc^{α} has been introduced into the solution for the friction coefficient.

We next define the quantity Δ as the ratio of the concentration boundary layer thickness to the momentum boundary layer thickness:

$$\Delta = \frac{\delta_c}{\delta}. \quad (16)$$

Combining equation (16) with equations (6) and (15) yields:

$$1 = \frac{n+3}{n+2} Sc^{\alpha} x \frac{d}{dx}(\Delta^{(n+2)/n}) + Sc^{\alpha}\Delta^{(n+2)/n}. \quad (17)$$

The solution of the above equation is simplified by setting $D = \Delta^{(n+2)/n}$ to yield the first order non-homogeneous linear differential equation:

$$\frac{n+2}{n+3} \frac{1}{Sc^{\alpha}} \frac{1}{x} = \frac{dD}{dx} + \frac{n+2}{n+3} \frac{D}{x} \quad (18)$$

having the solution

$$\Delta = \frac{\delta_c}{\delta} = \left\{\frac{1}{Sc^{\alpha}}\left[1 - \left(\frac{x_0}{x}\right)^{(n+2)/(n+3)}\right]\right\}^{n/(n+2)}. \quad (19)$$

Substituting equation (16) into equation (12) and combining with the expression for the friction coefficient (5), the local binary Stanton number becomes:

$$St_{AB_x} = \frac{1}{Sc^{(n+1)\alpha/(n+2)}} \left[\lambda^n \frac{(n+2)(n+3)}{n} Re_x\right]^{-2/(n+3)} \times \left[1 - \left(\frac{x_0}{x}\right)^{(n+2)/(n+3)}\right]^{-1/(n+2)}. \quad (20)$$

Thus, the use of α allowed the Schmidt number to remain as an integral part of the solution for the boundary layer ratio. The use of α also allowed the final expression of the local Stanton number to be expressed as a function of the Schmidt number. Notice as well that the power of the Schmidt number has become dependent on the profile power, n. The Schmidt number would not have appeared as an integral part of the solution had the Reynolds analogy been used.

The average mass transfer coefficient is found by integrating with:

$$\bar{h}_{mL} = \frac{1}{L - x_0} \int_{x_0}^{L} h_{mx}\, dx.$$

Solving for the local mass transfer coefficient from equation (17), and integrating to obtain the average mass transfer coefficient for a plate of length L and where x_0 is a starting distance at which sublimation begins, yields:

$$St_{AB_L} Sc^{(n+1)\alpha/(n+2)} = \frac{n+3}{n+1}\left[\lambda^n \frac{(n+2)(n+3)}{n}\right]^{-2/(n+3)} \times Re_L^{-2/(n+3)}\left[1 - \frac{x_0}{L}\right]^{-1} \times \left[1 - \left(\frac{x_0}{L}\right)^{(n+2)/(n+3)}\right]^{(n+1)/(n+2)}. \quad (21)$$

Equation (21) can be solved provided that n, α and λ are known. Both α and λ are assumed to be functions of n, and n is a function of the Reynolds number.

The turbulent boundary layer over a flat plate is similar in nature to that in pipe flow. In both cases, the boundary layer remains thin compared to the rest of the flow. In pipe flow, the boundary layer reaches the centerline when the flow becomes fully developed. Hence, due to the symmetry in fully developed pipe flow, the slope of the velocity profile at the centerline is zero. The slope of the velocity profile over a flat plate is also zero at the edge of the boundary layer. Therefore, it has been an established method to borrow the pipe flow $1/n$ power velocity profiles for flat plate boundary layer solutions. Prandtl first introduced this assumption which led to replacing the centerline velocity and radius in pipe flow by the free stream velocity and boundary layer thickness over the flat plate. This analogy is not exact because in a pipe the velocity distribution is due to a pressure gradient whereas the pressure gradient is zero over a flat plate [17].

Nikuradse [18] carried out experiments in which he was able to experimentally determine values of n for different Reynolds numbers in pipes. Table 1 lists Nikuradse's values of n at different Reynolds numbers with the pipe diameter as the characteristic length. A best fit equation for Nikuradse's data is:

$$\frac{1}{n} = 0.25654 - 2.4004 \times 10^{-2} \log_{10}(Re_L)$$

$$R^2 = 0.976. \quad (22)$$

In equation (22), the characteristic length has been changed from the pipe diameter to the distance downstream from the leading edge. This substitution was experimentally proven to be satisfactory [17].

Table 1. Values of n for different Reynolds numbers according to Nikuradse's experimental work

Re	4×10^3	2.3×10^4	1.1×10^5	1.1×10^6	2.0×10^6	3.2×10^6
n	6.0	6.6	7.0	8.8	10	10

The velocity coefficient and the Schmidt number power, λ and α, respectively, need to be related to n, and thus to the Reynolds number. Weighardt [19] determined values of λ for different values of n based on Nikuradse's data [17]. However, Kays and Crawford [14] suggest a value for λ of 8.75 at n equal 7 as opposed to Wieghardt's 8.74. In fractional form, 8.75 becomes:

$$8.75 = \frac{70}{8} = \frac{7\times10}{8} = \frac{7(7+3)}{(7+1)}.$$

Generalizing for any n yields:

$$\lambda(n) = \frac{n(n+3)}{(n+1)} \tag{23}$$

Table 2 compares Weighardt's values for λ with the values generated by equation (23). The percentage difference increases slightly with n. Both are empirical approximations. However, equation (23) provides the advantage of generating an infinite number of λ values for any real value of n as long as it is in the vicinity of 7. This assumption will be verified with the experimental data in the results.

Finally, α needs to be determined. For this purpose, and due to the similarities between heat and mass transfer, reference is made to the law of the wall for heat transfer in air [14]:

$$St = \frac{0.0287Re_x^{-0.2}}{0.169Re_x^{-0.1}(13.2Pr-10.16)+0.9} \quad \text{for } n = 7. \tag{24}$$

Equation (24) is valid for $0.5 < Pr < 1.0$ and $5\times10^5 < Re < 5\times10^6$. According to Kays and Crawford [11], the denominator in the above equation can be set approximately equal to:

$$0.169Re_x^{-0.1}(13.2Pr-10.16)+0.9 \approx Pr^{0.4} \quad \text{for } n = 7. \tag{25}$$

Therefore, equation (21) can be rewritten as:

$$St\,Pr^{0.4} = 0.0287Re_x^{-0.2} \quad \text{for } n = 7.$$

Using the analogy between heat and mass transfer, the Prandtl and Stanton numbers can be replaced by the Schmidt and the binary Stanton numbers respectively. Hence, the above equation becomes:

$$St_{AB_x}\,Sc^{0.4} = 0.0287Re_x^{-0.2} \quad \text{for } n = 7. \tag{26}$$

Therefore, from equation (21), the power of the Schmidt number can be set equal to 0.4 at n equal to 7. Hence:

$$0.4 = \frac{(7+1)\alpha}{7+2}.$$

Solving for α, and writing the solution in fractional form, yields:

$$\alpha = 0.45 = \frac{9}{2\times10} = \frac{7+2}{2(7+3)}.$$

Generalizing for any n, gives:

$$\alpha = \frac{n+2}{2(n+3)}. \tag{27}$$

Equation (27) yields a relationship between α and n based on a generalization of the above arithmetic solution for α. The need for such a generalization is due to the limitation of the arithmetic solution to $n = 7$. Equation (27) implies that α can be simply represented as function of n only. α's dependency on the Reynolds number is implied due to n's dependency on it. The validity of equation (27), as well as equations (22) and (23), will be verified by the correlation of the final solution to the data. Table 3 lists values of α and the power for the Schmidt number for different values of n. It can be seen that α is about 0.45 and the power of the Schmidt number is about 0.4.

Following is a summary of the solution for the $1/n$ power turbulent mass transfer from a flat plate in parallel flow with a step change in concentration. The average mass transfer coefficient, the average binary

Table 2. Comparison of the λ values generated by equation (19) to Weighardt's [17] values

n	λ (this study)	λ (Weighardt)	% difference
6	7.714	—	—
7	8.75	8.74	0.1144
8	9.778	9.71	0.6980
9	10.8	10.6	1.8867
10	11.818	11.5	2.7668

Table 3. Values of α and the Schmidt number power for different values of n

n	α	$\frac{(n+1)\alpha}{n+2}$
4	0.428 6	0.357 2
5	0.437 5	0.375 0
6	0.444 4	0.388 9
7	0.450 0	0.400 0
8	0.454 5	0.409 1

Stanton number, n as a function of the Reynolds number, and λ and α as a function of n are listed.

$$\bar{h}_{mL} = \frac{n+3}{n+1}\frac{v\,Sc^{-(n+1)\alpha/(n+2)}}{L-x_0}\left[\lambda^n\frac{(n+2)(n+3)}{n}\right]^{-2/(n+3)} \times Re_L^{(n+1)/(n+3)}\left[1-\left(\frac{x_0}{L}\right)^{(n+2)/(n+3)}\right]^{(n+1)/(n+2)}$$

$$St_{AB_L}\,Sc^{(n+1)\alpha/(n+2)} = \frac{n+3}{n+1}\left[\lambda^n\frac{(n+2)(n+3)}{n}\right]^{-2/(n+3)} \times Re_L^{-2/(n+3)}\left[1-\frac{x_0}{L}\right]^{-1}\left[1-\left(\frac{x_0}{L}\right)^{(n+2)/(n+3)}\right]^{(n+1)/(n+2)}$$

where

$$\frac{1}{n} = 0.256\,54 - 2.400\,4\times10^{-2}\log_{10}(Re_L)$$

and

$$\lambda(n) = \frac{n(n+3)}{(n+1)}$$

and

$$\alpha(n) = \frac{n+2}{2(n+3)}. \tag{28}$$

RESULTS AND DISCUSSION

Due to the empirical nature of the proposed solution, it was necessary to validate it by comparing it to mass transfer data. The apparatus and procedure described earlier were used for this purpose. The starting length for all tests was 5.08 cm (2″), the distance from the leading edge of the plate to the recess. The length of the cast naphthalene portion of the plate was varied by gluing an aluminum strip a certain distance downstream from the leading edge. Data were collected at the following four different naphthalene plate lengths as measured from the leading edge (i.e. the origin in Fig. 4):

$$L = \begin{cases} 64.8\,\text{cm}\ (25.5'') \\ 30.5\,\text{cm}\ (12.0'') \\ 25.4\,\text{cm}\ (10.0'') \\ 21.0\,\text{cm}\ (8.25'') \end{cases}.$$

The data collected are graphically represented in Fig. 5 as the Sherwood number vs the Reynolds number. The $1/n$ power solution discussed above is also graphed on the same figure. The Sherwood number is used to non-dimensionalize the mass transfer coefficient. It is defined as:

$$Sh = \frac{Sc\,\bar{h}_{mL}L}{v}. \tag{29}$$

All the data shown in Fig. 5 are within 10% of the Sherwood number predicted by the solution suggested in this study. The data collected covers a range of Reynolds numbers starting at approximately 40 000 and extending to 2 000 000. The two data points at the highest Reynolds numbers were underpredicted by 11.2 and 12.6%, respectively.

Based on the Sherwood number vs Reynolds number plot, agreement between the proposed solution and the data collected in this study can be established for Reynolds numbers ranging from 40 000 up to 1 500 000. Data up to a Reynolds number of 2 000 000 were collected: however, further testing is required to justify agreement at this range. The margin of error between the data and the proposed solution was generally within the random experimental error determined through a Kline–Mclintock experimental error analysis. The error equation for the Reynolds number is:

$$\frac{\delta Re}{Re} = \left[\left(\frac{1}{2}\frac{\delta h}{h}\right)^2 + \left(\frac{\delta L}{L}\right)^2\right]^{1/2}. \tag{30}$$

The error equation for the mass transfer coefficient is:

$$\frac{\delta\bar{h}_{mL}}{\bar{h}_{mL}} = \left\{\left(\frac{4\delta m}{m_{in}-m_f-(m_{int}-m_{ft})}\right)^2 + \left(\frac{\delta t}{t}\right)^2 + \left(\frac{\delta\mathscr{L}}{\mathscr{L}}\right)^2 + \left(\frac{\delta W}{W}\right)^2 + \left(\frac{\rho_{v_s}}{\rho_{v_s}-\rho_{v_\infty}}\right)^2 \times\left[\left(\frac{6713\ln(10)}{1.8T_{av}}\right)^2+1\right]\left(\frac{\delta T}{T_{av}}\right)^2 + \left(\frac{\rho_{v_\infty}}{\rho_{v_s}-\rho_{v_\infty}}\right)^2\left[\left(\frac{4\delta m}{m_{in}-m_f+(m_{int}-m_{ft})}\right)^2 + \left(\frac{\delta l}{l}\right)^2 + \left(\frac{\delta w}{w}\right)^2 + \left(\frac{\delta H}{H}\right)^2\right]\right\}^{1/2}. \tag{31}$$

And the error equation for the Sherwood number is:

$$\frac{\delta Sh}{Sh} = \left[\left(\frac{\delta\bar{h}_{mL}}{\bar{h}_{mL}}\right)^2 + \left(\frac{\delta\mathscr{L}}{\mathscr{L}}\right)^2\right]^{1/2}. \tag{32}$$

The respective errors were:

$$0.132\% < \frac{\delta Re}{Re} < 16.67\% \quad 1.038\% < \frac{\delta Sh}{Sh} < 8.02\%.$$

The data shown in Fig. 5 have an average error of -2.3% and a standard deviation of 5.6.

Velocity measurements were made just downstream of the leading edge of the plate from which it was concluded that the flow was turbulent over the entire naphthalene surface.

The use of a step discontinuity in sublimation allows for maintaining a sharp leading edge while having a surface that sublimes. Moreover, the location of the step change in this study was determined such that, in all trials, turbulent flow would exist at the beginning of the naphthalene surface. From a practical standpoint, the step discontinuity signifies the existence of a constant temperature heat sink or source away from the leading edge. It is also used for solving cases where

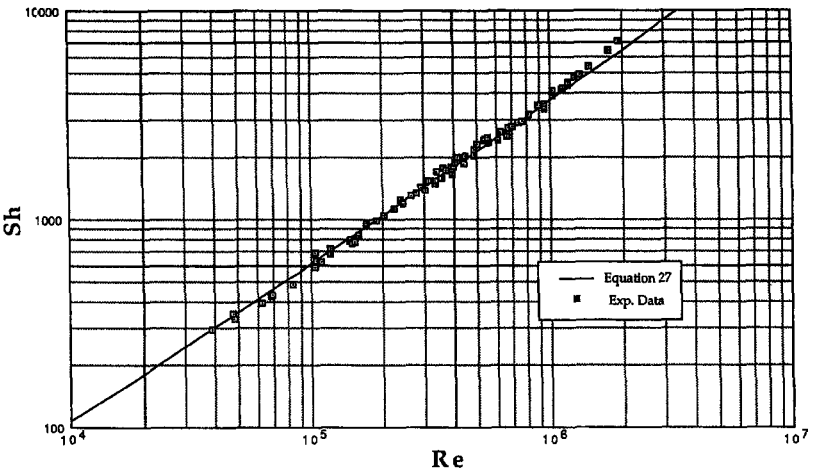

Fig. 5. Comparison of the experimental and theoretical Sherwood number vs the Reynolds number.

the temperature distribution over the plate has a certain distribution, the heat transfer from which can be more easily obtained by replacing the temperature distribution by a summation of a series of steps and solving.

CONCLUSIONS

A solution based on the $1/n$ power law was proposed such that the Reynolds analogy was circumvented by keeping the Schmidt number raised to a power α as an integral part of the solution. Expressions for the values of α and the coefficient for the power profile in terms of n were proposed. In addition, an empirical relationship relating n to the Reynolds number was obtained based on turbulent pipe flow. Agreement between the proposed solution and the data collected in this study was established for Reynolds numbers ranging from 40 000 up to 1 500 000. Data up to a Reynolds number of 2 000 000 were collected. It was found that the overall Sherwood number could be adequately predicted by equation (28) for Reynolds numbers ranging from 40 000 to 1 500 000 and Schmidt numbers from 1 to 2.5. The 1/7 power law consistently underpredicts the data by about 2.3% whereas the proposed method provides a better fit over the entire range, especially at Reynolds numbers over 100 000. It overpredicts the data by an average of 1.8%.

REFERENCES

1. D. S. Maisel and T. K. Sherwood, Evaporation of liquids into turbulent gas streams, *Chem. Engng Prog.* **46**(3), 131–138 (1950).
2. S. Scesa and F. M. Sauer, An experimental investigation of convective heat transfer to air from a flat plate with a stepwise discontinuous surface temperature, *Transactions of the ASME*, pp. 1251–1255 (October 1952).
3. T. K. Sherwood and H. S. Bryant, Jr, Mass transfer through compressible turbulent boundary layers, *Can. J. Chem. Engng* **35**, 51–57 (1957).
4. J. D. Anderson, Jr, *Fundamentals of Aerodynamics*. McGraw-Hill (1984).
5. H. H. Sogin, Laminar transfer from isothermal spanwise strips on a flat plate, *ASME J. Heat Transfer* **82**, 53–63 (1960).
6. H. H. Sogin and R. J. Goldstein, Turbulent transfer from isothermal spanwise strips on a flat plate, *Proceedings* 1961–1962 *ASME Heat Transfer Conference*, pp. 447–453 (1963).
7. W. C. Reynolds, Heat transfer in the turbulent incompressible boundary layer with constant and variable wall temperature, Ph.D. Thesis, Stanford University (1957).
8. P. H. Love, R. P. Taylor, H. W. Coleman and M. H. Hosni, Effects of thermal boundary condition on heat transfer in the turbulent incompressible flat plate boundary conditions, Report TFD-88-3, AFOSR-86-0178 (December 1988).
9. P. H. Love, R. P. Taylor, H. W. Coleman and M. H. Hosni, The effects of step changes in the thermal boundary condition on heat transfer in the incompressible flat plate turbulent boundary layer, *Proceedings of the* 1989 *National Heat Transfer Conference*, HTD-Vol. 107, *Heat Transfer in Convective Flows*, pp. 9–16 (1989).
10. R. P. Taylor, P. H. Love, H. W. Coleman and M. H. Hosni, Heat transfer measurements in the incompressible turbulent flat plate boundary layers with step wall temperature boundary conditions, *ASME J. Heat Transfer* **112**, 245–247 (1990).
11. Y. P. Chyou, The effect of a short unheated length and a concentrated heat source on the heat transfer through a turbulent boundary layer, *Int. J. Heat Mass Transfer* **34**, 1917–1928 (1991).
12. P. G. Huang, P. Bradshaw and T. J. Coakley, Skin friction and velocity profile family for compressible turbulent boundary layers, *AIAA J.* **31**, 1600–1604 (1993).
13. R. M. C. So, Pressure gradient effects on Reynolds analogy for constant property equilibrium turbulent boundary layers, *Int. J. Heat Mass Transfer* **37**, 27–41 (1994).
14. W. M. Kays and M. E. Crawford, *Convective Heat and Mass Transfer* (2nd Edn). McGraw-Hill (1980).
15. R. B. Bird, W. A. Stewart and E. N. Lightfoot, *Transport Phenomena*. Wiley (1960).
16. W. C. Reynolds, W. M. Kays and S. J. Kline, Heat transfer in the turbulent incompressible boundary layer. I—Constant wall temperature, NASA Memo 12-1-58W

(1958); and Heat transfer in the turbulent incompressible boundary layer. II—Step wall temperature distribution, NASA Memo 12-2-58W (1958).
17. H. Schlichting, *Boundary Layer Theory* (7th Edn). McGraw-Hill (1979).
18. J. Nikuradse, Gesettzmässigkeit der turbulenten Strömung in glatten Rohren, *Forsch. Arb. Ing.-Wes.* **356** (1932).
19. K. Wieghardt, Turbulente grenzschichten, Göttinger Monographie, Part B **5** (1946).